Stereochemical Outcome and Kinetic Effects of *R*p- and *S*p-Phosphorothioate Substitutions at the Cleavage Site of Vaccinia Type I DNA Topoisomerase†

James T. Stivers,*,‡ Barbara Nawrot,§ G. Jayashree Jagadeesh,‡ Wojciech J. Stec,§ and Stewart Shuman||

Center for Advanced Research in Biotechnology of the University of Maryland and the National Institute for Standards and Technology, 9600 Gudelsky Drive, Rockville, Maryland 20850, Department of Bioorganic Chemistry, Centre of Molecular and Macromolecular Studies, Polish Academy of Sciences, Lodz, Poland, and Molecular Biology Program, Sloan-Kettering Institute, New York, New York 10021

Received October 20, 1999; Revised Manuscript Received February 1, 2000

ABSTRACT: To probe the mechanism of the reversible DNA phosphodiester bond cleavage and religation mechanism of the type I topoisomerase from vaccinia virus, we have synthesized DNA substrates carrying a single nonbridging *R*p- or *S*p-phosphorothioate (Ps) modification at the scissile phosphodiester (Pd) bond. Analysis of the stereochemical outcome of the net cleavage and rejoining reaction established that the reaction proceeds with retention of configuration, as expected for a double-displacement mechanism. Single-turnover kinetic studies on irreversible strand cleavage using 18/24 mer suicide substrates showed thio effects (k^{Pd}/k^{Ps}) of 340- and 30-fold for the *R*p-Ps and *S*p-Ps stereoisomers, respectively, but ≈10-fold smaller thio effects for the reverse single-turnover religation reaction (*R*p-Ps = 30 and *S*p-Ps = 3). As compared to the smaller suicide cleavage substrates, approach-to-equilibrium cleavage studies using 32/32 mer substrates showed 7−9-fold smaller thio effects on cleavage, similar effects on religation, and the same ratio of the *R*p to *S*p thio effect as the suicide cleavage reaction (≈10). In general, thio effects of 2.4−7.2-fold on the cleavage equilibrium are observed for the wild-type and H265A enzymes, suggesting differences in the interactions of the enzyme with the nonbridging sulfur in the noncovalent and covalent complexes. Studies of the cleavage, religation, and approach-to-equilibrium reactions catalyzed by the H265A active site mutant revealed a stereoselective, 11-fold decrease in the *R*p-thio effect on cleavage and religation as compared to the wild-type enzyme. This result suggests that His-265 interacts with the nonbridging pro-*R*p oxygen in the transition state for cleavage and religation, consistent with the arrangement of this conserved residue in the crystal structure of the human topoisomerase−DNA complex. In general, the greatest effect of thio substitution and the H265A mutation is to destabilize the transition state, with smaller effects on substrate binding. The interaction of His-265 with the pro-*R*p nonbridging oxygen is inconsistent with the proposal that this conserved residue acts as a general acid in the strand cleavage reaction.

The vaccinia virus type IB topoisomerase catalyzes reversible site-specific cleavage and religation of the phosphodiester backbone of duplex DNA at CCCTT↓ sites using an active site tyrosyl residue as the nucleophile and the 5′-deoxyribose hydroxyl as the leaving group (Figure 1) (*1*). Type IB topoisomerases play an essential role in eukaryotic and mammalian DNA metabolism by allowing supercoiled DNA to "relax" around the swivel point generated by enzyme when it is covalently attached to a single strand of duplex DNA (*2*). In addition, the potentially powerful anticancer drug, camptothecin, selectively targets cellular type 1B enzymes by blocking the strand religation reaction (*3*). Thus, studies that identify and quantify the enzyme−substrate interactions that are involved in binding and catalysis are essential to fully elucidate the mechanism of these reactions.

The phosphodiester cleavage reactions of type I topoisomerases are unique in that the reaction is freely reversible and the energy of the initial DNA linkage is stored in the phosphotyrosyl covalent intermediate. Thus, single-turnover kinetic studies of cleavage and religation may be performed using reversible kinetic conditions or, alternatively, irreversible conditions (*4*). Using such approaches, kinetic studies on the strand cleavage and religation reactions of the vaccinia enzyme have been performed using small duplex oligonucleotide substrates (*4, 5*). These studies have indicated that the chemical step of cleavage was the slowest step in a single-turnover of the enzyme and that a simple two-state mechanism for cleavage and religation was sufficient to account for the observed kinetic results (Figure 1).[1] More recent

† This work was supported by the National Institute of Standards and Technology, NIH Grant GM46330 to S.S., and by Committee of Scientific Research Grant 4 P05F 006 17 to W.J.S.

* To whom correspondence and reprint requests should be addressed. Tel: 301-738-6264. FAX: 301-738-6255. E-mail: stivers@carb.nist.gov.

‡ Center for Advanced Research in Biotechnology of the University of Maryland and the National Institute for Standards and Technology.

§ Polish Academy of Sciences.

|| Sloan-Kettering Institute.

[1] In previous kinetic, pH−rate, and thio effect studies using a different set of substrates than used here, we inferred the existence of another conformational state of the covalent enzyme−DNA complex (*4*). However, this state was calculated to comprise less than 1% of the total enzyme bound DNA, and thus, the previous data were also compatible with a two-state equilibrium.

10.1021/bi992429c CCC: $19.00
Published on Web 04/13/2000

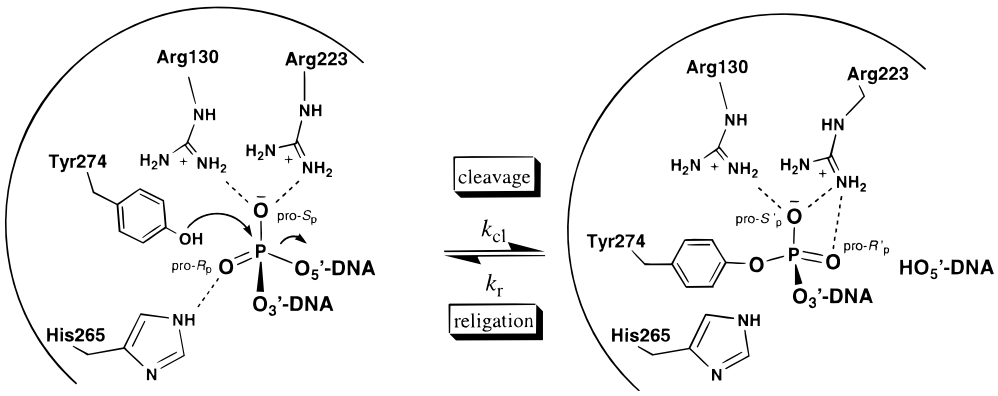

FIGURE 1: Interactions of the vaccinia type I topoisomerase with the scissile phosphodiester as inferred from the crystal structures of the covalent and noncovalent complexes of the human type I DNA topoisomerase (*9*). A direct in line displacement reaction is suggested in which the active site Tyr-274 attacks the scissile phosphodiester linkage, and the 5′-hydroxyl leaving group is expelled. The interactions of three key residues are indicated. His-265 forms a hydrogen bond (2.8 Å) to the pro-*R*p oxygen in the precleavage complex, and Arg-130 and Arg-223 form hydrogen bonds to the pro-*S*p oxygen (3.3 and 2.8 Å, respectively). In the covalent complex the residue corresponding to His-265 is disordered and not observed, Arg-223 forms a monodentate interaction with the both the pro-*S*′p and *R*′p oxygens (3.0 and 2.7 Å), and Arg-130 forms a monodentate interaction with the pro-*S*′p oxygen (2.8 Å). (In the text, we note the *R*p and *S*p configurations in the covalent complex with primes to emphasize that inversion of configuration has occurred compared to the precleavage complex.) Interestingly, directed mutagenesis studies have shown that Arg-130 is *not* replaceable by lysine, but the R223K mutant has similar activity to the wild-type enzyme (*5*, *36*). This result suggests that Arg-130 forms a bidentate interaction in transition state, which differs from the interaction of this residue in the structures of the human enzyme.

kinetic studies using supercoiled plasmid substrates were also consistent with rate-limiting cleavage chemistry and have established a "free rotation" mechanism for supercoil release by the vaccinia enzyme, in which multiple supercoils are removed for each cleavage and religation event (*6*).

A detailed structural model for the active sites of type IB enzymes has recently emerged from the crystal structures of the free vaccinia catalytic domain (*7*) and structures of the human enzyme in its noncovalent and covalent complexes with DNA (Figure 1) (*8*, *9*). From the structures of these complexes it is observed that two completely conserved arginine residues (Arg-130 and Arg-223 of the vaccinia enzyme) interact with the pro-*S*p oxygen of the scissile phosphodiester bond and that a conserved histidine residue (His-265 of the vaccinia enzyme) is within hydrogen-bonding distance of the pro-*R*p oxygen. The importance of these interactions in catalysis by the vaccinia enzyme has been directly demonstrated by site-directed mutagenesis studies. In this work, the R130A and R223A mutations caused a 10^5-fold inhibitory effect on the strand cleavage reactions (*5*, *10*−*12*), while the H265A and H265Q mutations caused a lesser 100- and 3-fold inhibitory effect, respectively (*13*). It has been proposed by Champoux and colleagues for the human enzyme that the histidine corresponding to His-265 acts as a general acid to protonate the 5′-hydroxyl leaving group in the strand cleavage reaction (*9*). However, the position of this histidine in the crystal structure, the "rescuing" effect of the vaccinia H265Q mutation as compared to the H265A substitution (*13*), and the results presented herein, suggest that the role of this histidine is to donate a neutral hydrogen bond to the pro-*R*p nonbridging oxygen in the transition state.

In an earlier paper (*5*), we showed that substitution of a *racemic* nonbridging phosphorothioate (Ps) linkage at the DNA cleavage site of the vaccinia enzyme resulted in biphasic cleavage kinetics. We suggested that the biphasic kinetic behavior was due to differing rates of cleavage for the two Ps diastereomers by the enzyme. Thus, these results suggested important stereospecific interactions of the enzyme with each nonbridging phosphoryl oxygen. In this paper, we further investigate this observation using chiral phosphorothioate substrates and directed mutagenesis in order to dissect the functional roles of the contacts to the individual phosphoryl oxygens at the cleavage site. Consistent with the previous biphasic kinetics, we find that *R*p-Ps substitution is about 10-fold more inhibitory than *S*p-Ps substitution and that the overall stereochemical outcome of the cleavage and religation reactions is net retention of configuration at phosphorus. For the H265A topoisomerase, a 11-fold decrease in the *R*p thio effect on cleavage and religation is observed as compared to the wild-type enzyme, indicating that His-265 interacts with the pro-*R*p oxygen in the transition state. This result suggests that His-265 is not a general-acid catalyst but, instead, acts to stabilize the developing negative charge on an equatorial oxygen in the transition state.

EXPERIMENTAL PROCEDURES[2]

Enzymes. Wild-type vaccinia topoisomerase was overexpressed from *Escherichia coli* strain BL21(DE3) transformed with the T7-based expression plasmid pET21-topo and purified to homogeneity using phosphocellulose chromatography as previously described (*14*), followed by an HPLC[3] gel filtration step using a Tosohaas TSK column (21.5 cm × 60 cm). The Y274F mutant was generated using the QuikChange double-stranded mutagenesis kit obtained from Stratagene (La Jolla, CA). The mutation was confirmed by DNA sequencing of both strands of the construct, and the expressed protein was purified in a fashion identical to that for the wild-type enzyme. The H265A mutant topoisomerase was expressed and purified as previously described (*13*). The concentration of the wild-type enzyme and the Y274F mutant were determined by UV absorption measurements at 280 nm (*5*), and the concentration of the H265A mutant was

[2] Certain commercial equipment, instruments, and materials are identified in this paper in order to specify the experimental procedure. Such identification does not imply recommendation or endorsement by the National Institute of Standards and Technology, nor does it imply that the material or equipment identified is necessarily the best available for the purpose.

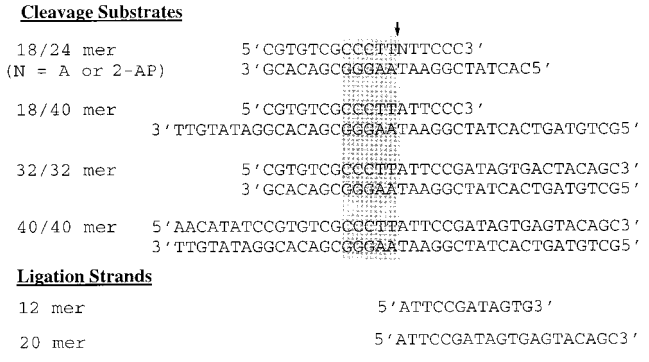

FIGURE 2: Sequences of the substrates used in this work. The conserved pentapyrimidine consensus sequence is aligned in all the substrates, and the scissile phosphodiester is marked with an arrow. The *R*p and *S*p phosphorothioate (Ps) substrates have a single sulfur substitution at the scissile position. In the sequence of the 18/24 mer, N = A or 2-aminopurine (2-AP).

determined by the Coomassie dye binding method (Bio-Rad, Hercules, CA) using wild-type topoisomerase as the standard. The enzymes snake venom phosphodiesterase, terminal deoxynucleotidyl transferase, nuclease P1, and alkaline phosphatase were obtained from Boehringer-Mannheim (Indianapolis, IN). T4 polynucleotide kinase was from New England Bio-Labs (Beverly, MA).

Oligonucleotide Substrates. The sequences of the phosphodiester and phosphorothioate substrates used in these studies are shown in Figure 2. The phosphodiester oligonucleotides were synthesized using standard phosphoramidite chemistry on an ABI 380B synthesizer (Applied Biosystems) at the 0.5−1.0 μmol scale. Stereospecific phosphorothioate substitutions were placed in the 18 mer oligonucleotides at the scissile phosphorus of the CCCTT$_{Ps}$A sequence by synthesis and block coupling of separately purified *R*p-T$_{Ps}$A and *S*p-T$_{Ps}$A dinucleotides by the methods previously described (*15*). The 18 mer Ps-oligonucleotides containing the fluorescent base, 2-aminopurine (2-AP), were synthesized using the commercially available 2-AP phosphoramidite reagent (Glen Research, Sterling, VA). A single phosphorothioate modification in the 2-AP-containing oligonucleotide was introduced at the CCCTT$_{Ps}$(2-AP) sequence using S-Tetra reagent (Glen Research, Sterling, VA), and the resulting *R*p and *S*p diasteromers were separated by RP-HPLC on a C18 column (Hypersil, 4.6 mm × 25 cm) using an acetonitrile (B) gradient in triethylammonium carbonate (1 M, pH 7.0) (A) as follows: 0 to 5 min, 0 to 25.5% B; 5 to 25 min, isocratic at 25.5% B; 25 to 28 min, 25.5% to 100% B.

The configuration and stereochemical purity of the Ps-oligonucleotides were determined by RP-HPLC of the free nucleosides after digestion with snake venom phosphodiesterase, nuclease P1, and alkaline phosphatase (*16*). The *R*p-Ps and *S*p-Ps oligonucleotides used in this work were of >99% stereochemical purity. Chemical purity and structural confirmation was determined by analytical RP-HPLC analysis on a Hypersil C18 column, electrophoresis using a denaturing 20 wt % polyacrylamide gel, and MALDI-TOF. The concentrations of the single-strand oligonucleotides were determined from the pairwise extinction coefficients at 260 nm of the individual nucleotides (*17*). The strands containing the scissile bond were 5′-^{32}P end-labeled using γ-^{32}P ATP in the presence of T4 polynucleotide kinase, purified on Biospin 6 columns (Bio-Rad, Hercules, CA), and then hybridized to the complementary strand supplied in a 3-fold excess. [The excess single strand DNA has no discernible effect on the reaction because the vaccinia enzyme does not have significant affinity for single strand DNA (*4*).] For determining the site of cleavage for the Pd, *R*p-Ps and *S*p-Ps 18/24 mer substrates, the 18 mer strands containing the scissile bond were 3′-^{32}P end-labeled using α-^{32}P ddATP in the presence of terminal deoxynucleotidyl transferase and then hybridized and purified as described above.

Determining the Stereochemistry of the Topoisomerase Reaction. The stereochemical outcomes of the net cleavage and religation reactions catalyzed by topoisomerase I using the *R*p-Ps and *S*p-Ps 18/40 mer substrates (Figure 2) were determined by taking advantage of the known stereospecificities of the enzymes snake venom phosphodiesterase (SVPDE) and nuclease P1 (NP1) (*16*). (For cleavage at phosphorothioate linkages, SVPDE cleaves *R*p-Ps and NP1 cleaves *S*p-Ps.) The detailed procedure is described in the legend of Figure 3.

2-Aminopurine Fluorescence Assay for Noncovalent DNA Binding. The noncovalent binding affinity of topoisomerase for the normal and Ps-substituted 18/24 mer duplexes containing the fluorescent reporter group 2-aminopurine (2-AP) 3′ to the cleavage site (Figure 2) was determined by monitoring the fluorescence intensity increase at 370 nm as the enzyme binds. To prevent cleavage of the DNA, the Y274F mutant topoisomerase was used in these measurements. Measurements were made using a Spex Fluoromax-2 fluorometer (ISA Instruments, Edison, NJ) with excitation at 315 or 320 nm, excitation and emission slit widths of 4 nm, and an emission scan range of 335−450 nm. These measurements were made using two different buffer conditions: 50 mM Tris-HCl (pH 7.5) and 20 mM Tris-HCl (pH 8.0) supplemented with 200 mM NaCl. Further details of the binding studies are described in the legend to Figure 6. The fluorescence data were fitted to eq 1, where F_o and F_f are the initial and final fluorescence values, respectively, and $b = K_D + [E]_{tot} + [DNA]_{tot}$.

$$F = F_o - [(F_o - F_f)/2[DNA]_{tot}\{b - \sqrt{b^2 - 4([E]_{tot}[DNA]_{tot})}\}] \quad (1)$$

Single-Turnover Cleavage Kinetics. Cleavage experiments were performed with the 18/24 mer substrates (see Figures 2 and 4) using single-turnover conditions with manual or machine mixing using a Kin-Tek rapid chemical-quench flow apparatus (State College, PA). In these experiments, the enzyme was always present in at least 5-fold excess over the DNA so that the observed kinetics were pseudo-first-order. For the manual experiments, 10 μL of DNA (0.1−50 nM) in 50 mM Tris-HCl buffer (pH 7.5) was placed in 10 separate wells of a 96-well microtiter plate with V-bottoms.

[3] Abbreviations: HPLC, high performance liquid chromatography; Tris-HCl, tris(hydroxymethyl)aminomethane; SDS, sodium dodecyl sulfate; SDS−PAGE, polyacrylamide gel electrophoresis in the presence of the denaturant SDS; EDTA, (ethylenedinitrilo)tetraacetic acid, disodium salt; 2-AP, 2-aminopurine; Pd, phosphodiester; Ps, phosphorothioate; MALDI, matrix-assisted laser desorption−ionization mass spectrometry; SVPDE, snake venom phosphodiesterase; NP1, nuclease P1.

To initiate a reaction, 10 μL of wild-type or H265A topoisomerase (0.5 to 1.2 μM)) in 50 mM Tris-HCl buffer (pH 7.5) was rapidly added with a P-10 pipetman (Rainin, Woburn, MA). The reaction was quenched by the addition of 20 μL of 2X SDS quench solution, which was rapidly dispensed from a second hand-held pipet. The quench times ranged between 0.5 and 10 s, and accurate timing was achieved with an electronic metronome as previously described (*6*). Control experiments demonstrated that the addition of 1 volume of 10 wt % SDS was an efficient quench method and that the co-addition of glycerol and bromphenol blue had no effect on the results. For the machine mix experiments, ~30 μL of a 1 μM topoisomerase solution was mixed with an equal volume of DNA (20 nM) and the reactions were quenched at times ranging from 0.1 to 10 s with a solution of 10 wt % SDS delivered from the quench syringe. After quenching, glycerol and bromophenol blue were added to each reaction to final concentrations of 5 and 0.1 wt %, respectively. The reaction products were analyzed by separating the free uncleaved DNA from the covalently bound DNA using electrophoresis with a 18 wt % denaturing polyacrylamide gel containing SDS. The fraction of the uncleaved substrate remaining (frac S_t) was determined by phosphorimaging analysis and corrected for the amount of substrate that did not react at long times (frac S_∞): frac $(S_t)_{norm}$ = (frac S_t − frac S_∞)/(1 − frac S_∞). The data were fitted to a first-order decay curve [frac $(S_t)_{norm} = \exp -k_{obsd}t$] by nonlinear regression analysis. Similar to previous results (*4*), the corrections for unreactive substrate ranged from 5 to 25%. In multiple experiments it was found that the observed rate constant (k_{obsd}) for a given substrate did not depend on the fraction of the substrate that was unreactive at long times. The enzyme concentration dependence of the single-turnover cleavage rates (k_{obsd}) was fitted to eq 2 to obtain the maximal cleavage rate at saturating enzyme concentration (k_{cl}) and the apparent dissociation constant (K_D^{app}).

$$k_{obsd} = k_{cl}[E]/[E] + K_D^{app} \quad (2)$$

The precise site of cleavage for the Pd and *R*p- and *S*p-Ps 18/24 mer substrates was determined using 3′-α^{32}P ddATP end-labeled DNA (see above). The 7 mer products of the cleavage reaction were then resolved on a denaturing 20% polyacrylamide gel containing 7 M urea.

Single-Turnover Religation Kinetics. The rates of 20 mer strand religation to preformed 5′-^{32}P-labeled enzyme−12/40 mer covalent complexes were determined under single-turnover irreversible conditions using manual or machine mixing methods. The manual reactions (20 μL each in 50 mM Tris-HCl, 0.3 M NaCl, pH 7.5) were performed in 96-well microtiter plates as described above for the cleavage reactions. The covalent complex between wild-type topoisomerase and the *R*p-Ps and *S*p-Ps 18/40 mer DNA was first formed in 50 mM Tris-HCl buffer (150 μL, pH 7.5) by incubating 0.65 μM wild-type topoisomerase with 50 nM DNA for 2 h. The 10 μL portions of the preformed complexes were then dispensed into 10 separate wells of a microtiter plate. The religation reactions were initiated by the rapid addition of 10 μL of a 2× ligation mix consisting of 40 μM 20 mer strand in a buffer consisting of 0.6 M NaCl in 50 mM Tris-HCl (pH 7.5). The machine mixing experiments were performed by mixing a 30 μL solution of preformed covalent complex (~50 nM) with a 40 μM solution of 20 mer (in 50 mM Tris-HCl, 0.6 M NaCl). Thus, the final conditions at the initiation of the reactions were ~25 nM covalent complex, 20 μM 20 mer strand, and 50 mM Tris-HCl containing 0.3 M NaCl at pH 7.5. (The presence of 0.3 M NaCl makes the religation reaction irreversible by preventing reassociation of the topoisomerase with the DNA.) The manual and machine initiated reactions were quenched as described for the cleavage reactions, and the covalent complex and 32/40 mer ligation product were resolved by electrophoresis using a 18 wt % polyacrylamide gel using denaturing conditions (SDS−PAGE).

The religation reactions of the H265A topoisomerase with the normal, *R*p-Ps. and *S*p-Ps 18/40 mers were performed in a similar fashion except that (i) the time scale for forming the respective E−12/40 mer covalent complexes was longer (Pd, 4 h; *R*p-Ps, 24 h; *S*p-Ps, 48 h) and (ii) a single 300 μL reaction was used from which 20 μL aliquots were removed and quenched in 20 μL of the 2× SDS quench solution (see above). After electrophoresis, the fraction of the covalent complex remaining (frac complex_t = $(\text{counts complex})_t$/{[counts 32/40 mer]$_t$ + [counts complex]$_t$}) was determined by phosphorimaging analysis of the gels and then corrected for the amount of covalent complex that did not react at long times (frac complex_∞): frac $(\text{complex}_t)_{norm}$ = (frac complex_t − frac complex_∞)/(1 − frac complex_∞). The data were fitted to a first-order decay curve [frac $(\text{complex}_t)_{norm} = \exp -k_r t$] using nonlinear regression analysis. Further details of the individual reactions are in the legend to Figure 7.

Approach-to-Equilibrium Cleavage Kinetic Measurements. Approach-to-equilibrium kinetic measurements were performed using 40/40 mer or 32/32 mer substrates with 20 base pairs 3′ to the cleavage site, such that the leaving strand cannot spontaneously dissociate (Figure 2). The 5′-^{32}P-labeled 32 mer scissile strand was synthesized by first end-labeling the respective normal, *R*p-Ps, and *S*p-Ps 18 mer strands with γ^{32}P-ATP in the presence of T4 polynucleotide kinase and then hybridizing these labeled strands to the complementary 32 mer which was present in a 3-fold molar excess (bottom strand in Figure 2). The labeled 18 mer strand was ligated to a 14 mer oligonucleotide (5′-ATAGTGACTACAGC-3′) in the presence of ATP and T4 DNA ligase, which results in the 32/32 mer duplex shown in Figure 2. The labeled duplex was resolved on a 20 wt % nondenaturing polyacrylamide gel and then excised and electroeluted to give pure material for the reactions. The reactions were performed and analyzed as described above for the single-turnover cleavage reactions using manual mixing for the *R*p-Ps and *S*p-Ps substrates, and machine mixing for the reaction of the wild-type enzyme with the normal 40/40 mer. The observed rate constant for approach-to-equilibrium cleavage (k_{obs}^{rev}) was obtained from plots of the fraction of substrate cleaved against time using nonlinear least-squares fitting to a first-order rate equation (frac cleaved = $\text{frac}_\infty(1 - \exp -k_{obs}^{rev}t)$, where frac_∞ is the amount of substrate cleaved at infinite time (i.e. when equilibrium has been reached).

RESULTS

Net Cleavage and Religation Reaction Proceeds with Retention of Configuration at Phosphorus. The overall

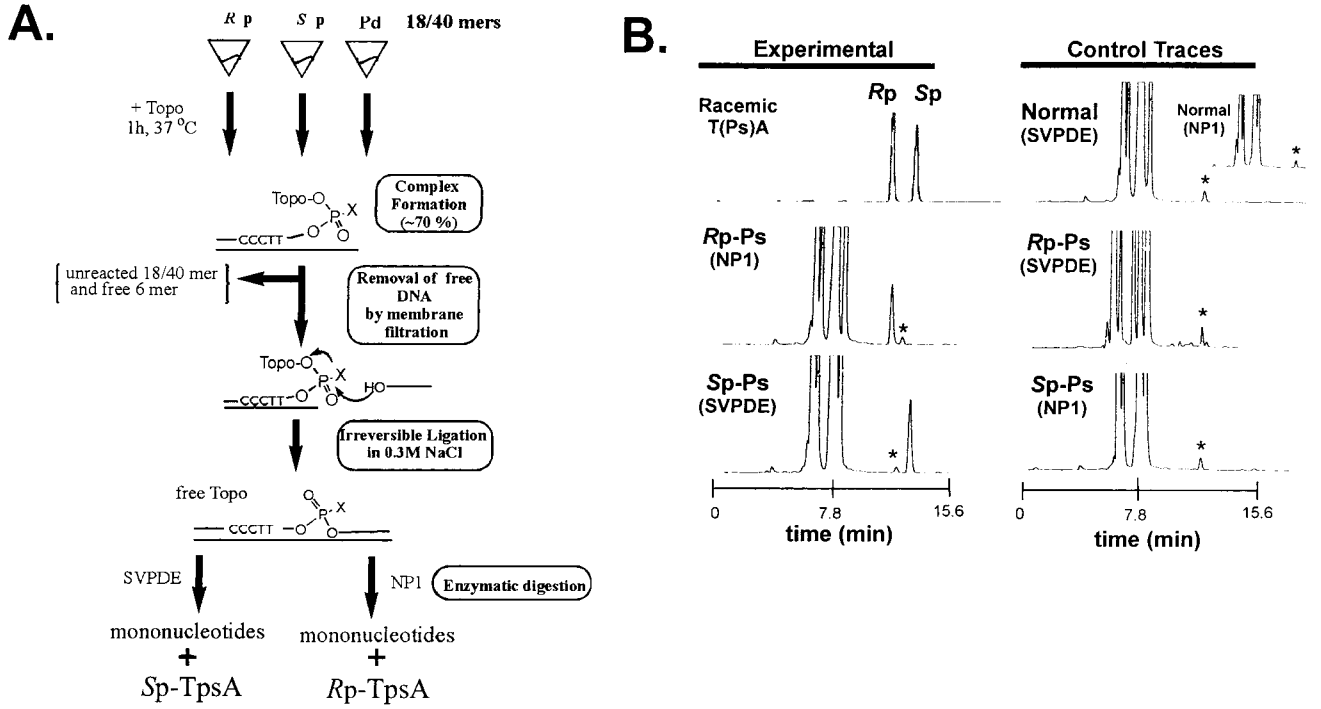

FIGURE 3: Determination of the stereochemical outcome of the net cleavage and religation reactions. (A) Three 100 μL reactions containing 10 μM of either the *R*p, *S*p, or normal 18/40 mer and 16 μM topoisomerase in a buffer consisting of 50 mM Tris-HCl (pH 7.5) were incubated at 37 °C for 1 h to form the covalent complex. The reactions were then diluted 150-fold to a volume of 15 mL using 50 mM Tris-HCl containing 0.3 M NaCl. The samples were placed in three Amicon (Beverly, MA) Centriprep-30 membrane filtration devices and concentrated to a volume of about 1 mL (MWCO = 30 000). The samples were diluted to 15 mL and concentrated again to 1 mL by centrifugation. Finally, the 1 mL retentate was transferred to a Amicon Centricon-10 membrane filtration device, and the volume was reduced to about 100 μL. (At this stage, which represents an overall dilution of 2250-fold, the unreacted 18/40 mer DNA and the free 6 mer leaving strand were not detected in the retentate by analysis using denaturing 20% polyacryamide gel electrophoresis with visualization by UV shadowing or ethidium bromide staining.) The ligation reaction was initiated by addition of the 12 mer strand (see Figure 2) to a final concentration of about 30 μM, and the reaction was incubated for 1 h at room temperature. (Under these high-salt conditions, ligation is essentially irreversible because the topoisomerase dissociates irreversibly from the DNA.) After ligation, the buffer was exchanged by diluting each of the three reactions to 2 mL using 10 mM K_2HPO_4 (pH 7.3) and 10 mM $MgCl_2$ and then concentrating each sample to 100 μL using a Centricon-3 device. Finally, each of the three samples was split into two equal-volume portions, to which 10 U of SVPDE was added to one and 10 U of NP1 to the other. After addition of 10 U of alkaline phosphatase to all the samples, they were incubated at room temperature for 48 h. (B) The nucleoside and phosphorothioate $T_{Ps}A$ dimer products for the reaction were analyzed by RP-HPLC using a Phenomenex C18 Aqua column (Torrance, CA) with UV monitoring at 254 nm. An isocratic elution scheme was used consisting of 0.1 M aqueous triethylammonium acetate with 14 vol % acetonitrile, and a flow rate of 0.5 mL/min. The stereochemical assignments of the dimers from these digestions were confirmed with the chemically synthesized *R*p and *S*p dimers of $T_{Ps}A$. The asterisk marks an impurity that is present in all the samples.

reaction catalyzed by type I topoisomerases is envisioned to proceed by a double-displacement mechanism involving (i) the nucleophilic attack of the active site tyrosine on the scissile phosphodiester to form a phosphotyrosine covalent intermediate and (ii) the attack of the DNA 5′-hydroxyl on the phosphotyrosine intermediate to reseal the DNA strand. Thus, the expected overall stereochemical outcome is retention of configuration at phosphorus. To directly confirm this mechanistic prediction, we placed a chiral *R*p- or *S*p-phosphorothioate linkage at the cleavage site, isolated the product of the overall topoisomerase reaction (Figure 3A), and determined the stereochemical configuration at the scissile linkage using the well-known stereospecificities of the enzymes snake venom phosphodiesterase (cleaves only *R*p-Ps) and nuclease P1 (cleaves only *S*p-Ps). Thus, the expected enzymatic digestion products (after removal of the 5′-phosphate with bacterial alkaline phosphatase) are the four mononucleosides and a single dinucleotide with a chiral phosphorothioate linkage ($T_{Ps}A$) that is resistant to digestion by the given enzyme. The HPLC traces in Figure 3B clearly show that the $T_{Ps}A$ dinucleotide products derived from the *R*p-Ps and *S*p-Ps 18/40 mer substrates retain the *R*p and *S*p configuration, respectively. On the basis of the signal-to-noise level in the HPLC traces, it can be estimated that the net cleavage and religation reaction proceeded with greater than 97% retention of configuration at phosphorus.

Thio Effects on the Irreversible Single-Turnover Cleavage Reactions of Wild-Type and H265A Topoisomerase. The reversible nucleophilic substitution reaction of the vaccinia topoisomerase may be studied under irreversible cleavage conditions using substrates which are incapable of being ligated. One way to accomplish this is to use duplex oligonucleotides with less than 6 base pairs 3′ of the cleavage site, such that the 6 mer irreversibly dissociates after the cleavage reaction (Figure 4) (*4*). For the wild-type enzyme, the Pd−18/24 mer is cleaved with a maximal rate constant $k_{cl} = 0.67$ s^{-1} (Figure 4A, Table 1). The substitution of *R*p-Ps and *S*p-Ps at the cleavage site results in large stereospecific thio effects on k_{cl} of 340- and 30-fold, respectively (Figure 4B, Table 1).

To rigorously interpret the observed thio effects on k_{cl}, it is necessary to ascertain that the site of cleavage has not been altered by the introduction of sulfur at the scissile position. To establish this point, we labeled the scissile strand

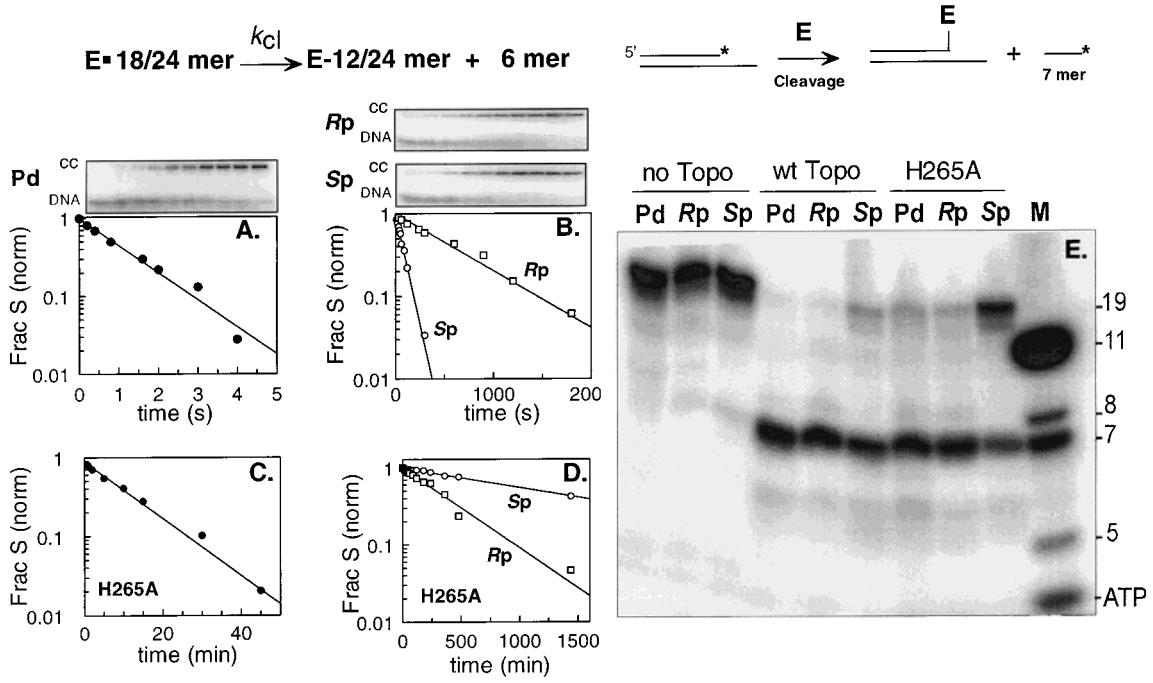

FIGURE 4: Maximal single-turnover cleavage rates for the 18/24 mer Pd and Ps duplexes under irreversible conditions and determination of the site of cleavage. The reactions were performed by rapidly mixing equal volumes of enzyme and DNA and quenching the reaction at various times by the addition of 1 volume of 10 wt % SDS. The data are shown as semilogarithmic plots and are normalized for the fraction of the substrate that did not react at long times. (A) Reaction of wild-type topoisomerase (600 nM) with the Pd 18/24 mer (performed with a Kin-Tek rapid mix−quench instrument). The last time point shown in the gel (10 s) was used to determine the endpoint and is not shown in the plot. (B) Reaction of the wild-type topoisomerase (600 nM) with the *R*p- and *S*p-Ps 18/24 mer substrates. In the gel images, the time points range from 10 to 1800 s (*R*p) and 10 to 300 s (*S*p), and the last point in each was used to determine the end point and is not plotted. (C, D) Reactions of Pd, *R*p, and *S*p 18/24 mers with the H265A mutant (300 nM). (E) The site of cleavage for the Pd and Ps substrates was ascertained by 3′-end-labeling the 18 mer scissile strand with α^{32}P-ddATP followed by hybridization to the complementary 24 mer strand. The labeled DNA (20 nM) was incubated with 100 nM wild-type or H265A topoisomerase for about 5 h at 37 °C in a reaction volume of 20 μL, and the reaction products were resolved on a 20% denaturing polyacrylamide gel containing 7 M urea. The unreacted DNA is shown in the three lanes on the left, and reactions of the wild-type and H265A enzymes with the Pd and Rp- and Sp-Ps substrates are shown moving from left to right across the gel. In all cases, the major reaction product is the expected 3′-end-labeled 7 mer, as judged by comigration with the 3′-end-labeled 7 mer marker band. The cleavage reaction of the Sp diastereomer with the H265A enzyme is only partially complete at 5 h due to the long half-life of this reaction (Table 1).

Table 1: Kinetic Parameters and Thio Effects for Wild-Type and H265A Topoisomerase[a]

substrate	k_{cl} (s^{-1})	TE^{cl}	k_r (s^{-1})	TE^r	K_D^{app} [b] (nM)
			Wild-Type		
Pd	0.67 ± 0.10		0.90 ± 0.10		19 ± 4
*R*p-Ps	0.002 ± 0.0004	340	0.03 ± 0.003	30	≤ 1
*S*p-Ps	0.021 ± 0.0006	30	0.29 ± 0.018	3	3 ± 1
			H265A		
Pd	$(1.2 \pm 0.1) \times 10^{-3}$		$(2.0 \pm 0.15) \times 10^{-3}$		5 ± 2
*R*p-Ps	$(4.0 \pm 0.3) \times 10^{-5}$	30	$(7.3 \pm 0.5) \times 10^{-4}$	2.6	ND[c]
*S*p-Ps	$(1.2 \pm 0.1) \times 10^{-5}$	100	$(2.0 \pm 0.2) \times 10^{-4}$	10	ND

[a] Determined at 25 °C and pH 7.5 (50 mM Tris-HCl). The thio effect (TE) is defined as Pd value/Ps value, and the superscript denotes the corresponding rate constant or equilibrium constant. The values for k_{cl} and k_r were determined from single-turnover kinetic measurements as described in the text using irreversible conditions. In general, the reported rate constants are mean values for two to four independent determinations, and the errors are standard uncertainties. The propagated errors in the thio effects are ≤20%. [b] The apparent dissociation constant determined from the concentration dependence of k_{obsd} for single-turnover cleavage (see eq 2 and Figure 5). Thio effects on this parameter are not reported because the K_D^{app} value for the Pd substrate with the wild-type enzyme is higher than the true K_D due to kinetic complexity (see text). [c] ND, not determined.

of each 18/24 mer substrate with α^{32}P-ddATP using terminal deoxynucleotidyl transferase and resolved the cleavage products of the reactions on a denaturing 20% polyacrylamide gel containing 7 M urea. If cleavage occurs at the expected position, then each of the substrates should be converted to 7 mers in these reactions. As shown in Figure 4E, the 3′-end-labeled scissile strands with a Pd, *R*p-Ps, or *S*p-Ps linkage are each converted to the expected 7 mer product as judged by oligonucleotide size markers which were included on the gel.

To determine whether thio substitution affects the affinity of the enzyme for these substrates, we investigated the enzyme concentration dependence of k_{obsd} (eq 2) for the single-turnover suicide cleavage reaction (Figure 5A,B). For the wild-type enzyme reacting with the 18/24 mer Pd substrate, an apparent dissociation constant for cleavage (K_D^{app}) of 19 nM was determined by nonlinear least-squares fitting of the concentration dependence of k_{obsd} to eq 2 (Figure 5B). For the *R*p- and *S*p-Ps 18/24 mers, much lower K_D^{app} values of ≤ 1 and 3 nM were measured, respectively (inset,

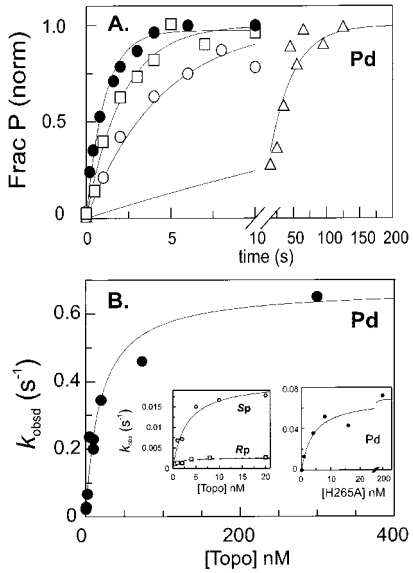

FIGURE 5: Concentration dependence of single-turnover strand cleavage of the Pd and Ps 18/24 mer substrates (50 mM Tris-HCl, pH 7.5). (A) Varying concentrations of enzyme (1−300 nM) were mixed with 0.2 nM of the Pd 18/24 mer. The amount of covalent complex at each time was quantified as described in the legend to Figure 4 and in the Experimental Procedures, and the time courses were fitted to a first-order rate equation to obtain k_{obsd} at each concentration of enzyme. The concentrations of enzyme for the data shown are the following: closed circles, 300 nM; squares, 50 nM; open circles, 10 nM; triangles, 1 nM. (B) Concentration dependence of k_{obsd} for cleavage of the Pd 18/24 mer and Ps 18/24 mers by the wild-type topoisomerase (inset) and Pd 18/24 mer by the H265A mutant (inset) The curves are nonlinear least-squares fits of the data to eq 2, from which the values for k_{cl} and K_D^{app} reported in Table 1 were determined.

Figure 5B). Although these results seem to indicate that the introduction of sulfur significantly *increases* the affinity of the enzyme for the *R*p- and *S*p-Ps substrates, an alternative explanation would be that K_D^{app} for the Pd substrate is greater than the true dissociation constant because of kinetic complexity. Using the minimal cleavage mechanism of eq 3, K_D^{app} could overestimate K_D^{true} by the ratio of the rate

$$E + S \underset{k_{-1}}{\overset{k_1}{\leftrightarrow}} ES \xrightarrow{k_{cl}} E{-}S \qquad (3)$$

constants k_{cl}/k_1 (i.e. $K_D^{app} = K_D^{true} + k_{cl}/k_1$) (*18*). Thus, the much larger k_{cl} value for the Pd substrate could give rise to its higher K_D^{app}. The similarity of the K_D values for the Pd, *R*p-Ps, and *S*p-Ps substrates determined in direct binding studies using the Y274F mutant support this explanation (see below).

We note that the cleavage reaction of the Pd−18/24 mer has been followed from times as short as 5 ms and using enzyme concentrations ranging from 1 to 600 nM and that no kinetic lags have been detected. This is an important observation, because if cleavage occurs by a two-step mechanism involving a slow conformational step followed by chemistry as previously suggested (*1*), a pronounced lag in covalent complex formation should have been detected if the conformational step was 3−10-fold slower than the chemical step (*18*). In general, such a lag will not be observed if the first step of a two-step reaction is much faster or slower than the second step. Thus, the absence of a detectable lag indicates that any conformational change that may be occurring must operate at a rate >10-fold faster or slower than the subsequent chemical step. We note that the 11-fold *smaller* thio effect on cleavage for the H265A mutant is also inconsistent with a rate-limiting conformational change that obscures the chemical step, because the rate of the chemical step is slowed by 560-fold by the H265A mutation (see below).

Table 2: H265A Mutational Effects (ME) on Cleavage and Religation[a]

substrate	ME^{cl}	ME^{r}	ME_{kobs}^{rev}	ME^{Kcl}
Pd	560	480	230	0.78
*R*p-Ps	50	41	26	2.4
*S*p-Ps	1700	1500	900	2.3

[a] The fold mutational effects on cleavage (ME^{cl}), religation (ME^{r}), reversible cleavage (ME_{kobs}^{rev}), and the cleavage equilibrium constant (ME^{Kcl}) for each substrate are reported as fold effects between the wild-type and H265A mutant topoisomerases (i.e. ME = wild-type value/H265A value), and the propagated errors are less than 30%. The mutational effects are calculated from the data in Tables 1 and 3.

For the H265A topoisomerase, the maximal cleavage rates for the Pd, *R*p-Ps, and *S*p-Ps 18/24 mers were down by 560-, 50-, and 1700-fold, respectively, as compared to the wild-type enzyme (Figure 4C,D and Table 2). The *R*p-Ps thio effect on the cleavage reaction of the H265A topoisomerase is 11-fold *smaller* than the wild-type enzyme, while the effect of *S*p-Ps substitution is 3-fold greater than the effect measured for wild-type topoisomerase. This stereospecific "rescuing" effect of the H265A mutation provides evidence for a favorable interaction of His-265 with the pro-*R*p nonbridging oxygen. The K_D^{app} for cleavage of the Pd 18/24 mer by the H265A mutant was also in the low nanomolar range (K_D^{app} = 5 nM, Figure 5), as found for the cleavage of the *R*p- and *S*p-Ps substrates by the wild-type enzyme. It was not practical to measure K_D^{app} for cleavage of the *R*p- and *S*p-Ps substrates by the H265A mutant due to the extremely slow rates of these reactions (Table 1).

Noncovalent DNA Binding. The overall binding interaction of the topoisomerase with DNA may be viewed as a two-step process involving first the formation of a noncovalent complex, described by a dissociation constant K_D, followed by a reversible covalent step, described by the cleavage equilibrium constant K_{cl}. To evaluate the effect of nonbridging phosphorothioate substitutions on K_D, we used the Y274F active site mutant, which is incapable of forming the covalent complex yet binds productively as judged by DNA footprinting analysis of the vaccinia enzyme (*19*), and the crystal structure of the analogous human Phe mutant in a noncovalent complex with DNA (*8*). In a new assay for binding (Figure 6), a 2-aminopurine fluorescent reporter group (**P**) is placed adjacent to the consensus cleavage sequence CCCTT↓**P**. Thus, upon noncovalent binding of the Y274F enzyme, a 1.9−2.4-fold fluorescence enhancement is observed for the Pd− and Ps−18/24 mer substrates (Figure 6A, 6B). Because 2-aminopurine fluorescence is quenched dramatically by base stacking interactions in duplex DNA (*20, 21*), the observed enhancement is presumably due to a decrease in the stacking interactions of the 2-aminopurine base upon noncovalent binding of the enzyme.

Using the standard reaction buffer (50 mM Tris-HCl, pH 7.5), we were only able to observe tight stoichiometric binding of the Y274F mutant to the Pd− and Ps−18/24 mers

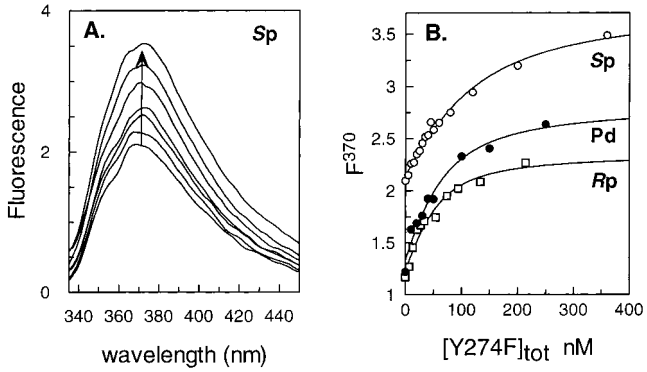

FIGURE 6: Determination of the noncovalent binding affinity of Y274F topoisomerase for the normal and Ps-substituted 18/24 mer duplexes in the high ionic strength buffer (20 mM Tris-HCl, 200 mM NaCl at pH 8.0). The substrates contain the fluorescent reporter group 2-aminopurine (**P**) at the position 3′ to the cleavage site, which results in a fluorescence increase upon noncovalent binding. (A) Fluorescence emission spectra (λ_{ex} = 320 nm) of the *S*p-Ps substrate DNA (89 nM) as the topoisomerase concentration is increased from 0 to 350 nM. (B) Relative fluorescence increase at 370 nm for the Pd substrate (50 nM, closed circles), *R*p-Ps substrate (50 nM, open squares), and *S*p-Ps substrate (89 nM, open circles) as a function of total Y274F enzyme concentration. The curves are the best fits to eq 1. From this analysis, the K_D values for the respective Pd, *R*p-Ps, and *S*p-Ps 18/24 mer substrates are 36 ± 17, 23 ± 12, and 70 ± 16 nM. As discussed in the text, the k_{cl} values in this buffer are nearly the same as those in the low ionic strength standard buffer, indicating that productive complexes are being formed in this experiment.

using this assay ($K_D \leq 4$ nM, $n = 1 \pm 0.1$, data not shown), which is consistent with low nanomolar dissociation constants for all these substrates in the standard buffer (i.e. $K_D^{app} \gg K_D$ for the Pd substrate as suggested above). A better determination of the K_D values using this buffer system was precluded by the sensitivity of the fluorescence assay. Therefore, to obtain a better measure of the relative binding affinities of the enzyme for the Pd and Ps substrates, we increased the ionic strength of the assay buffer to include 200 mM NaCl and 20 mM Tris-HCl, pH 8.0. In this buffer system, K_D values of 36 ± 17, 23 ± 12, and 70 ± 16 nM were measured for the Pd, *R*p-Ps, and *S*p-Ps 18/24 mers, respectively, by curve fitting the concentration dependence of the fluorescence increases to eq 1 (Figure 6B). To confirm that catalytically productive complexes form in this higher salt buffer, the cleavage rates were measured at a saturating concentration of enzyme ([E] = 1 or 2 μM, [18/24 mer] = 20 nM) and were found to be very similar to those measured in the standard low ionic strength buffer: $k_{cl}^{Pd} = 0.59 \pm 0.05$ s^{-1}; $k_{cl}^{Rp} = 0.003 \pm 0.0006$ s^{-1}; $k_{cl}^{Sp} = 0.016 \pm 0.003$ s^{-1}. These results indicate that sulfur substitution has only a small effect on substrate affinity (≤2-fold) and support the proposal that the larger K_D^{app} value for cleavage of the Pd substrate is due to kinetic complexity (Figure 5; see also discussion above).

Thio Effects on the Single-Turnover Religation Reactions of Wild-Type and H265A Topoisomerase. The single-turnover religation reaction may also be studied using irreversible conditions. In this case, the E−12/40 covalent complex is first formed from the 18/40 mer substrate, and religation is then initiated by the rapid addition of a large excess of 20 mer strand that is complementary to the single-strand overhang of the complex (Figure 7). To make religation

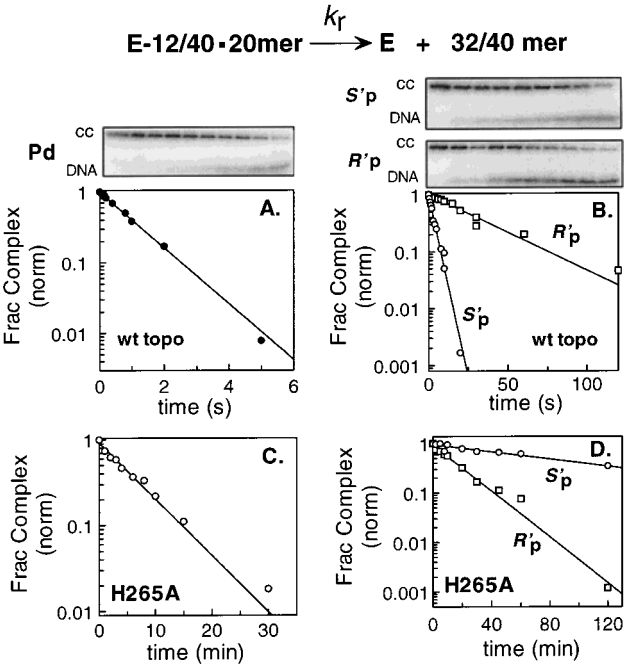

FIGURE 7: Single-turnover religation of Pd and Ps E−12/40 covalent complexes (cc) with 20 mer religation strand under irreversible conditions. The designations *R*′p and *S*′p reflect the fact that the stereochemical configuration at phosphorus for the covalent complex is inverted with respect to the precleavage complex. The data are fitted to a single-exponential decay and are displayed in semilogarithmic plots, normalized for the fraction of the initial complex that did not react at long times (see text and Figure 4). (A) Reaction of the wild-type Pd covalent complex with the ligation strand (performed with machine mixing). (B) Reaction of the wild-type *R*′p and *S*′p-Ps covalent complexes with 20 mer ligation strand. (C) Reaction of H265A−Pd covalent complex with 20 mer ligation strand. (D) Religation reactions of H265A−*R*′p and H265A−*S*′p-Ps covalent complexes.

irreversible, the reaction is performed in 300 mM NaCl, which drives enzyme dissociation from the DNA after religation. Although the higher salt concentration used for the religation reaction could affect the religation rate constant as compared to the standard buffer, the following observations indicate that salt effects on the religation rates are small: (i) the small effect of 200 mM NaCl on the maximal cleavage rates for the reaction of the Pd and Ps substrates with the wild-type enzyme; (ii) the similar religation rates for the Pd substrates obtained from reversible and irreversible religation measurements with the wild-type enzyme (compare k_r and k_r^{calc} in Tables1 and 3); and (iii) the good agreement between the thio effects on religation determined for the two approaches (Tables 1 and 3). Because the rates for reversible and irreversible religation for the Ps substrates show modest differences (20−80%), we do not make quantitative comparisons between the data obtained using these differing conditions for the Ps substrates.

For the wild-type enzyme, the E−12/40 mer covalent complex is ligated to form the 32/40 mer product with a rate constant $k_r = 0.90$ s^{-1} (Figure 7A, Table 1). The substitution of *R*p-Ps and *S*p-Ps at the cleavage site results in thio effects of 30- and 3-fold for k_r, respectively, which are roughly 10-fold less than the effects on k_{cl} (Figure 7B, Table 1). As discussed above for the cleavage reactions, religation occurs with no lags, indicating no other kinetically significant steps before the chemical step of ligation.

Table 3: Kinetic Parameters for Approach-to-Equilibrium Cleavage and Thio Effects (TE)[a]

substrate	k_{obs}^{rev} (s^{-1})	$TE^{obs,rev}$	K_{cl}	TE^{Kcl}	k_{cl}^{calc} [b]	$TE^{cl}{}_{calc}$ [c]	k_r^{calc} [b]	$TE^{r}{}_{calc}$ [c]
				Wild-Type				
Pd	1.3 ± 0.2		0.56 ± 0.06		0.5 ± 0.10		0.8 ± 0.14	
*R*p-Ps	0.029 ± 0.0035	45	0.52 ± 0.05	1.1	0.01 ± 0.002	50	0.019 ± 0.004	42
*S*p-Ps	0.36 ± 0.04	3.6	0.23 ± 0.04	2.4	0.07 ± 0.01	7.1	0.29 ± 0.03	2.7
				H265A				
Pd	$(5.7 \pm 0.7) \times 10^{-3}$		0.72 ± 0.1		$(2.4 \pm 0.3) \times 10^{-3}$		$(3.3 \pm 0.5) \times 10^{-3}$	
*R*p-Ps	$(1.1 \pm 0.1) \times 10^{-3}$	5	0.22 ± 0.04	3.3	$(2 \pm 0.3) \times 10^{-4}$	12	$(9 \pm 0.9) \times 10^{-4}$	3.7
*S*p-Ps	$(4.0 \pm 0.3) \times 10^{-4}$	14	0.1 ± 0.02	7.2	$(3.6 \pm 0.7) \times 10^{-5}$	67	$(3.6 \pm 0.3) \times 10^{-4}$	9.2

[a] The kinetic (k_{obs}rev) and equilibrium (K_{cl}) parameters are from the approach-to-equilibrium kinetic experiments in which the DNA was fully bound by enzyme ([E] = 300−600 nM, [DNA] = 20 nM). The thio effect (TE) is defined as Pd value/Ps value, and the superscript denotes the corresponding rate constant or equilibrium constant. In general, the errors in k_{obsd} and K_{cl} are standard uncertainties based upon multiple determinations of these parameters ($n = 2-4$). [b] The values k_{cl}^{calc} and k_r^{calc} were calculated from the kinetic equations describing a simple two-state approach-to-equilibrium for each substrate [i.e. $k_{cl}^{calc} = k_{obs}^{rev}/(1 + 1/K_{cl})$ and $k_r^{calc} = k_{obs}^{rev}/(1 + K_{cl})$]. [c] These thio effects were obtained from the *calculated* values of k_{cl} and k_r reported in this table; the propagated errors are ≤30%.

For the H265A topoisomerase, the religation rates for the Pd, *R*p-Ps, and *S*p-Ps E−12/40 mer complexes were down by 480-, 41-, and 1500-fold, respectively, as compared to the wild-type enzyme (Figure 7C,D, and Table 2). These fold effects of the H265A mutation on k_r are nearly identical to the mutational effects on k_{cl} for each of these substrates (Table 2). Since there is little mutational effect on K_{cl} (≤2.4-fold; see below and Table 2), then the large kinetic effects suggest that removal of His-265 destabilizes the transition state for cleavage and religation, with little effect on the relative free energy levels for the respective ground states. The *R*p-Ps and *S*p-Ps thio effects on the religation reaction catalyzed by the H265A topoisomerase are 11-fold smaller and 3-fold greater than those measured for the wild-type topoisomerase, respectively (Table 1). These changes in the thio effects upon mutation of His-265 are similar to those observed for k_{cl}, and indicate that His-265 has an identical role in the transition state for cleavage and religation (i.e. the same rate-limiting transition state is observed for both reactions).

Kinetics of DNA Cleavage and Religation Using Reversible Approach-to-Equilibrium Conditions. An alternative method for measuring DNA cleavage is to use reversible approach-to-equilibrium conditions (*4*). In these reactions, a longer substrate with 20 base pairs 3′ to the cleavage site is used such that the cleaved strand does not dissociate from the complex. Under such reversible conditions, and when the DNA is fully bound by enzyme, the equilibrium end point will depend on the relative rate constants for strand cleavage and religation (i.e. $K_{cl} = k_{cl}/k_r$) (*4*, *5*). Accordingly, the observed rate constant for reversible cleavage (k_{obs}^{rev}) is expected to be greater than the irreversible cleavage measurements and will be equal to the sum $k_{cl} + k_r$ for a simple two-state mechanism in which cleavage and religation occur through a single transition state (Figure 1) (*18*). Accordingly, k_{cl} and k_r may be calculated from k_{obs}^{rev} and K_{cl} by simultaneous solution of the two equations (see k_{cl}^{calc} and k_r^{calc} values in Table 3). For such a mechanism, we note that the thio effect on k_{obs}^{rev} ($TE^{obs,rev}$), will differ from the thio effect on suicide cleavage and religation according eq 4,

$$TE^{obs,rev} = \frac{(1 + 1/K_{cl}{}^{Pd})}{[1/TE^{cl} + (1/K_{cl}{}^{Pd} \times 1/TE^{r})]} \qquad (4)$$

where TE^{cl}, TE^{r}, and $K_{cl}{}^{Pd}$ are the thio effects on the individual rate constants k_{cl}^{calc} and k_r^{calc} and the cleavage equilibrium constant for the phosphodiester substrate, respectively. (Equation 4 may be easily derived from the equations defining k_{obs}^{rev}, K_{cl}, and the thio effect.)

For the wild-type enzyme, the Pd−40/40 mer is cleaved under reversible conditions with a maximal pseudo-first-order rate constant $k_{obs}^{rev} = 1.3 \pm 0.2\ s^{-1}$ and a cleavage equilibrium constant $K_{cl} = 0.56$ (Table 3, data not shown). As observed for the irreversible cleavage reaction, no kinetic lag was observed that would indicate a slow step before the chemical step. In addition, we note that k_{obs}^{rev} and K_{cl} for the Pd substrate are within error of the values calculated from the sum and ratio of k_{cl} and k_r, respectively (see Table 1), providing evidence that a simple two-state approximation is valid for this reaction. The calculated rate constants for cleavage (k_{cl}^{calc}) and religation (k_r^{calc}) obtained from the equations describing a two-state mechanism are reported in Table 3.

The substitution of *R*p-Ps and *S*p-Ps at the cleavage site of the 32/32 mer equilibrium cleavage substrate results in thio effects of 45- and 3.6-fold for k_{obs}^{rev}, respectively, and smaller effects on K_{cl} (1.1- and 2.4-fold; see Table 3). Although k_{obs}^{rev} is nearly identical to the sum k_{cl} and k_r for the Ps substrates (see Table 1), the ratio k_{cl}/k_r is about 7- and 3-fold greater than K_{cl} for the *R*p- and *S*p-Ps substrates, respectively. This result indicates that sulfur substitution has differential effects on the reactivity of the equilibrium and irreversible substrates, thus precluding any comparison of the cleavage and religation rates between these substrates using the two-state approximation (see Discussion). The *R*p and *S*p thio effects that are obtained from k_{cl}^{calc} and k_r^{calc} are reported in Table 3.

For the H265A topoisomerase, the Pd−40/40 mer is cleaved under reversible conditions with a maximal rate constant that is 230-fold slower than the wild-type enzyme, with a slightly larger equilibrium endpoint ($K_{cl} = 0.7$, Table 3). The thio effect on k_{obs}^{rev} for the H265A mutant is diminished by about 10-fold for the *R*p-Ps 32/32 mer as compared to the wild-type enzyme and increased by about 3-fold for the *S*p-Ps isomer, which is the same result obtained for the irreversible cleavage and religation reactions. As compared to the wild-type enzyme, larger thio effects on K_{cl} of 3.3 and 7.2 are seen for the *R*p and *S*p isomers, respectively (Table 3). These equilibrium thio effects indicate that the relative free energy levels for the noncovalent and covalent complexes have been altered as a result of mutation

and thio substitution so as to favor the noncovalent complex. Similar to the wild-type enzyme, the ratio k_{cl}/k_r for the *R*p- and *S*p-Ps substrates are 4- and 1.7-fold less than the measured values of K_{cl}, respectively. The *R*p and *S*p thio effects that are obtained from k_{cl}^{calc} and k_r^{calc} are reported in Table 3.

The concentration dependence of covalent complex formation was found to be similar for the Pd and Ps equilibrium cleavage substrates using the wild-type enzyme or the H265A mutant (not shown). Attempts to obtain a K_D value for noncovalent binding by following the concentration dependence of covalent complex formation were unsuccessful due to tight stoichiometric binding in the standard low ionic strength buffer (see above), as well as the small values of K_{cl} for the H265A mutant. However, for both the wild-type and H265A enzymes an upper limit $K_D \leq 5$ nM for the Pd and Ps 32/32 mer substrates was obtained from these studies using the standard buffer, which once again indicates that the high K_D^{app} value for the wild-type enzyme is due to kinetic complexity.

DISCUSSION

Stereochemistry. To our knowledge, the results reported here represent the first direct measurements of the stereochemical outcome of a type 1B topoisomerase reaction (Figure 3), although the stereochemistry of the related enzyme, lambda integrase, has been shown to proceed by retention of configuration (*22*). The observation of net retention of configuration is consistent with a double-displacement mechanism involving the formation of a phosphotyrosine intermediate, followed by attack of the 5′-hydroxyl group to reseal the phosphodiester backbone. Thus, it may be concluded that no stable trigonal bipyramidal intermediate exists with a significant lifetime to allow pseudorotation of the axial and apical phosphorus ligands and that no odd number of displacements has occurred.

Role for His-265 in the Topoisomerase Mechanism. The crystal structure of the homologous human type 1B topoisomerase noncovalently bound to DNA indicates that the nonbridging pro-*R*p oxygen forms a hydrogen bond (2.8 Å) with the H^{ϵ} proton of the histidine residue corresponding to His-265 of the vaccinia enzyme and Arg-130 and Arg-223 hydrogen bond with the pro-*S*p oxygen (Figure 1). In the structure of the covalent complex, this histidine is disordered and not observed, and Arg-223 forms a monodentate interaction with both nonbridging oxygens (3.0 and 2.7 Å), while Arg-130 forms a 2.8 Å hydrogen bond to the pro-*S*p′ oxygen. (Oxygens in the covalent complex are denoted with primes to emphasize that the stereochemical configuration at phosphorus is inverted with respect to the noncovalent complex.) Thus, these structures indicate that His-265 interacts with the pro-*R*p oxygen in the ground-state pre-cleavage complex and may interact weakly, or not at all, in the ground-state covalent complex.

Taken together, the effects of the H265A mutation on K_D^{app}, k_{cl}, k_r, and K_{cl} reported in Tables 1−3 indicate that the removal of His-265 has a small effect on the relative ground-state free energy levels of the noncovalent and covalent complexes but has a large damaging effect ($\Delta\Delta G$) in the range 14−16 kJ/mol on the free energy barrier for approach-to-equilibrium cleavage, suicide cleavage, and religation [$\Delta\Delta G = -RT$ ln(fold mutational effect)$^{-1}$; see Table 2]. Histidine-265 is conserved in all type 1B topoisomerases (*13*), as well as the mechanistically and structurally related HP1 and lambda integrase enzymes (*23*, *24*) and the XerD recombinase (*25*−*27*). Thus a common role for this residue in the transesterification reactions of these related enzymes is suggested (*10*).

The 11-fold smaller *R*p thio effect on irreversible cleavage and religation when using the H265A mutant enzyme strongly supports the structural evidence that His-265 forms a hydrogen bond to the pro-*R*p oxygen in the transition state for cleavage and religation, although indirect effects of mutations on thio effects have also been reported (*28*, *29*). Assuming a direct interaction, as suggested by the crystal structure, this "rescuing" effect of the H265A mutation corresponds to a favorable energetic coupling between His-265 and the pro-*R*p-oxygen in the transition state of −6 kJ/mol [the coupling or interaction energy (ΔG_{int}) may be calculated from the ratio of thio effects for the mutant (TE^{mut}) and wild-type enzymes (TE^{wt}), i.e., $\Delta G_{int} = -RT$ ln(TE^{wt}/TE^{mut})] (*30*, *31*). In contrast, the *S*p-Ps diastereomer shows a 3−10-fold *larger* thio effect with the H265A mutant than with the wild-type enzyme (Tables 1 and 3), which corresponds to an indirect, anticooperative energetic coupling between His-265 and the pro-*S*p oxygen in the transition state of 3.0 kJ/mol. These effects suggest a finely tuned and cooperative hydrogen bond network in the transition state that facilitates changes in geometry and charge as the tyrosine nucleophile attacks the phosphodiester linkage.

We surmise that His-265 is neutral in the DNA complex at pH 7.5 because the low activity of the Ala-265 enzyme is largely restored upon introduction of Gln at this position and the analogous residue in Cre-recombinase is a tryptophan (*25*). Thus, we propose that His-265 serves as a neutral hydrogen bond donor to the pro-*R*p oxygen and, therefore, does not serve as a general acid catalyst for expulsion of the 5′ hydroxyl leaving group as previously suggested for the corresponding His-632 of the human enzyme (*9*).

Catalytic Interactions with the Nonbridging Oxygens in the Transition State for Suicide Cleavage. The 2-AP fluorescence assay for binding indicates that sulfur substitution has ≤2-fold effect on the ground-state interactions of the enzyme with the Pd and Ps 18/24 mer substrates using the high ionic strength conditions in which the K_D values can be determined (Figure 6). Thus, for the wild-type enzyme, the large 340-fold *R*p thio effect on suicide cleavage must be attributed primarily to transition-state destabilization. This thio effect corresponds to an increase in the free energy barrier for cleavage of about 15 kJ/mol attributed to *R*p-Ps substitution ($=-RT$ ln $k_{cl}Rp/k_{cl}^{Pd}$), which is significantly reduced to about 9 kJ/mol for the H265A mutant. The 6 kJ/mol smaller effect for the mutant once again indicates that the catalytic benefit of the hydrogen bond between His-265 and the pro-*R*p oxygen has already been lost due to deletion of the imidazole side chain, such that further introduction of the *R*p-Ps substituent has a smaller damaging effect on catalysis. The large effect of *R*p-Ps substitution in the wild-type enzyme may be explained by the inability of the active site to accommodate the bulkier sulfur substituent in the expanded trigonal bipyramidal geometry of the transition state (*32*), the weaker hydrogen-bonding ability of sulfur as compared to oxygen, or its lower electronegativity (*33*).

As compared to *R*p sulfur substitution, the *S*p-Ps diastereomer shows a much smaller 9 kJ/mol effect on the free energy barrier for suicide cleavage, which *increases* to about 12 kJ/mol upon deletion of His-265. Although such changes are difficult to interpret with certainty, the smaller damaging effect of *S*p-Ps as compared to *R*p-Ps for the wild-type enzyme could result from *S*p-Ps substitution directing the longer $P-S^-$ bond toward Arg-130 and Arg-223, which may provide favorable Coulombic interactions that are offset by unfavorable steric and geometric clashes in the transition state. Alternatively, these results could reflect reduced steric effects for *S*p-substitution as compared to the *R*p-Ps diastereomer. The larger *S*p thio effect upon removal of His-265 could indicate that this residue helps position the *S*p substituent such that Arg-130 and Arg-223 can form favorable Coulombic interactions in the transition state (*34*). Accordingly, when the positioning provided by His-265 is removed by mutation, the damaging effect is greater for the *S*p sulfur because the interaction with a full negative charge is disrupted, whereas, for oxygen, a lesser damaging effect is realized because only a partial negative charge is involved in the interaction. Of course, other more complicated explanations for these effects are also possible.

Comparison with Previous Kinetic Results. The results reported here are in reasonable agreement with previous findings on the vaccinia enzyme and the H265A variant (*4*, *13*). These include (i) the observation of large stereospecific thio effects on the cleavage reaction, with one isomer reacting 1 order of magnitude more slowly than the other (*4*), (ii) the observation of a much smaller thio effect on the religation reaction as compared to cleavage (*5*), and (iii) similar measured values of k_{cl}, k_r, and K_{cl} for the H265A topoisomerase and the identical value of k_r for the wild-type enzyme as previously determined (*4*, *13*). As pointed out previously (*6*), the smaller suicide cleavage substrates that were used in our initial kinetic investigations of the vaccinia enzyme had slower rates of cleavage than the optimal substrates used here, which are cleaved at a rate that is kinetically competent to account for the observed rates of cleavage of supercoiled plasmid DNA ($0.3\ s^{-1}$) (*6*).

One notable observation in the current findings is that the fraction covalent complex trapped at equilibrium is about 2-fold larger than previous studies by Petersen and Shuman using a 60 mer cleavage substrate at 37 °C (*13*) and 4-fold larger than previous measurements with a 25 mer duplex substrate at 25 °C (*4*). The previous 60 mer has an identical sequence for 20 base pairs either side of the cleavage site as the 40/40 mer and 32/32 mer used in this work, while the previous 25 mer differs both in sequence and in position of the cleavage site as compared to the present substrates. Such sequence and position effects on K_{cl} for the vaccinia enzyme are not surprising, given that (i) differing amounts of covalent complex are trapped at different CCCTT sites within pUC19 supercoiled DNA (*6*) and (ii) recent results on a related pox virus topoisomerase showed a significant effect of the DNA flanking sequence on the cleavage equilibrium (*35*). One implication of these qualitative findings is that sequence specific substrate interactions distant from the cleavage site may be used to alter the relative free energy levels of the noncovalent and covalent complexes. Thus, the factors that determine the magnitude of the cleavage equilibrium constant are not well understood and merit further study.[4]

Why Are the Thio Effects Smaller for Religation? Since the results indicate that topoisomerase cleavage and religation of DNA can be approximated by a two-state mechanism, then the damaging effect of thio substitution (or mutagenesis) should be identical in the forward and reverse directions if the effect was solely on the transition state, and not the ground-state free energy levels for the noncovalent and covalent complexes. Thus, the small effect of the H265A mutation and *R*p thio substitution on the cleavage equilibrium, in combination with the large kinetic effects, indicates that for these substitutions the damaging effect is primarily due to transition-state destabilization. In contrast, the significant thio effects on the cleavage equilibrium for the reaction of the *S*p isomer with wild-type enzyme, and for the reactions of the *R*p and *S*p isomers with the H265A enzyme, indicate that sulfur substitution has increased the free energy level of the covalent complex relative to the noncovalent complex. This destabilization of the covalent complex due to thio substitution acts to reduce the activation barrier for religation as compared to cleavage, resulting in smaller thio effects on religation.

In previous work, using different substrates than used here, we had proposed that the smaller thio effect for religation was due to a partially rate-limiting conformational step, and sparsely populated intermediate, that obscured the thio effect on the chemical step of religation (see footnote 1) (*5*). Although this explanation is still formally possible, and may still hold for the previous substrates, the above results suggest an alternative explanation in which the different thio effects on cleavage and religation are due to differential changes in the relative free energy barriers for cleavage and religation as a result of different interactions of the enzyme with sulfur in the covalent and noncovalent complexes. We also suggest that the larger thio effect on suicide cleavage as compared to equilibrium cleavage results from differences in the enzyme interactions with the different DNA substrates used for these reactions.

Conclusions. This work provides a complete thio effect analysis of the reversible phosphoryl transfer reactions catalyzed by the vaccinia type 1B topoisomerase. The thio effects, in combination with directed mutagenesis and the structural information on the precleavage and covalent complexes, provide a reasonably consistent view of the interactions that are involved in catalysis. The thio effect and mutagenesis results indicate that His-265 plays an important role in stabilizing the negative charge on an equatorial oxygen in the trigonal bipyramidal transition state but does not act as the general acid to protonate the 5′-hydroxyl leaving group. The question whether another as of yet unidentified residue serves as the general acid remains to be established.

[4] It is common in the topoisomerase literature to use 1% by weight SDS as the equilibrium quench, as compared to the 5% quench used here. This more dilute quench solution may introduce additional errors in the estimation of K_{cl} at some cleavage sites because control experiments have shown that the amount of wild-type covalent complex that is trapped increases by a factor of 2 when the SDS concentration increases from 1% to 5 wt % (not shown). No further increase was observed when the SDS concentration was increased to 10 wt % in separate experiments conducted at 22 and 37 °C or when a Kin-tek rapid mixing device was used to quench the reaction on a millisecond time scale. Thus low concentrations of SDS do not serve as an efficient quench at some cleavage sites.

REFERENCES

1. Shuman, S. (1998) *Biochim. Biophys. Acta 1400*, 321−37.
2. Champoux, J. J. (1990) in *DNA Topology and its Biological Effects*, Cold Spring Harbor Laboratory Press, Cold Spring Harbor, NY.
3. Pommier, Y., Pourquier, P., Fan, Y., and Strumberg, D. (1998) *Biochim. Biophys. Acta 1400*, 83−105.
4. Stivers, J. T., Shuman, S., and Mildvan, A. S. (1994) *Biochemistry 33*, 327−39.
5. Stivers, J. T., Shuman, S., and Mildvan, A. S. (1994) *Biochemistry 33*, 15449−58.
6. Stivers, J. T., Harris, T. K., and Mildvan, A. S. (1997) *Biochemistry 36*, 5212−22.
7. Cheng, C., Kussie, P., Pavletich, N., and Shuman, S. (1998) *Cell 92*, 841−50.
8. Redinbo, M. R., Stewart, L., Kuhn, P., Champoux, J. J., and Hol, W. G. (1998) *Science 279*, 1504−13.
9. Stewart, L., Redinbo, M. R., Qiu, X., Hol, W. G., and Champoux, J. J. (1998) *Science 279*, 1534−41.
10. Wittschieben, J., and Shuman, S. (1997) *Nucleic Acids Res. 25*, 3001−8.
11. Wittschieben, J., and Shuman, S. (1994) *J. Biol. Chem. 269*, 29978−83.
12. Cheng, C., Wang, L. K., Sekiguchi, J., and Shuman, S. (1997) *J. Biol. Chem. 272*, 8263−9.
13. Petersen, B. O., and Shuman, S. (1997) *J. Biol. Chem. 272*, 3891−6.
14. Morham, S. G., and Shuman, S. (1992) *J. Biol. Chem. 267*, 15984−92.
15. Lesser, D. R., Grajkowski, A., Kurpiewski, M. R., Koziolkiewicz, M., Stec, W. J., and Jen-Jacobson, L. (1992) *J. Biol. Chem. 267*, 24810−8.
16. Eckstein, F., and Gish, G. (1989) *Trends Biochem. Sci. 14*, 97−100.
17. Fasman, G. D. (1975) in *Handbook of Biochemistry, Nucleic Acids*, 3rd ed., CRC Press, Boca Raton, FL.
18. Johnson, K. A. (1992) in *The Enzymes*, Vol. XX, pp 1−61, Academic Press, Orlando, FL.
19. Shuman, S. (1991) *J. Biol. Chem. 266*, 11372−9.
20. Stivers, J. T. (1998) *Nucleic Acids Res. 26*, 3837−3844.
21. Stivers, J. T., Pankiewicz, K. W., and Watanabe, K. A. (1999) *Biochemistry 38*, 952−963.
22. Mizuuchi, K., and Adzuma, K. (1991) *Cell 66*, 129−40.
23. Hickman, A. B., Waninger, S., Scocca, J. J., and Dyda, F. (1997) *Cell 89*, 227−37.
24. Kwon, H. J., Tirumalai, R., Landy, A., and Ellenberger, T. (1997) *Science 276*, 126−31.
25. Guo, F., Gopaul, D. N., and van Duyne, G. D. (1997) *Nature 389*, 40−6.
26. Gopaul, D. N., Guo, F., and Van Duyne, G. D. (1998) *EMBO J. 17*, 4175−87.
27. Yang, W., and Mizuuchi, K. (1997) *Structure 5*, 1401−6.
28. Hondal, R. J., Bruzik, K. S., Z., Z., and Tsai, M.-D. (1997) *J. Am. Chem. Soc. 119*, 5477−5478.
29. Hondal, R. J., Zhao, Z., Riddle, S. R., Kravchuk, A. V., Liao, H., Bruzik, K. S., and Tsai, M.-D. (1997) *J. Am. Chem. Soc. 119*, 9933−9934.
30. Mildvan, A. S., Weber, D. J., and Kuliopulos, A. (1992) *Arch. Biochem. Biophys. 294*, 327−40.
31. Zhang, Y.-L., Hollfielder, F., Gordon, S. J., Chen, L., Keng, Y.-F., Wu, L., Herschlag, D., and Zhang, Z.-Y. (1999) *Biochemistry 38*, 12111−12123.
32. Polesky, A. H., Dahlberg, M. E., Benkovic, S. J., Grindley, N. D., and Joyce, C. M. (1992) *J. Biol. Chem. 267*, 8417−28.
33. Frey, P. A., and Sammons, R. D. (1985) *Science 228*, 541−5.
34. Koziolkiewicz, M., and Stec, W. J. (1992) *Biochemistry 31*, 9460−6.
35. Hwang, Y., Burgin, A., Jr., and Bushman, F. (1999) *J. Biol. Chem. 274*, 9160−8.
36. Klemperer, N., and Traktman, P. (1993) *J. Biol. Chem. 268*, 15887−99.

BI992429C